NRC Research Press

ARTICLE

A stochastic mixed integer program to model spatial wildfire behavior and suppression placement decisions with uncertain weather

Erin J. Belval, Yu Wei, and Michael Bevers

Abstract: Wildfire behavior is a complex and stochastic phenomenon that can present unique tactical management challenges. This paper investigates a multistage stochastic mixed integer program with full recourse to model spatially explicit fire behavior and to select suppression locations for a wildland fire. Simplified suppression decisions take the form of "suppression nodes", which are placed on a raster landscape for multiple decision stages. Weather scenarios are used to represent a distribution of probable changes in fire behavior in response to random weather changes, modeled using probabilistic weather trees. Multistage suppression decisions and fire behavior respond to these weather events and to each other. Nonanticipativity constraints ensure that suppression decisions account for uncertainty in weather forecasts. Test cases for this model provide examples of fire behavior interacting with suppression to achieve a minimum expected area impacted by fire and suppression.

Key words: multistage stochastic programming, wildfire growth, wildfire suppression, uncertain fire weather.

Résumé : Le comportement des feux de forêt est un phénomène complexe et stochastique qui peut présenter des défis de gestion tactique particuliers. Cet article porte sur l'utilisation de la programmation stochastique multiétape partiellement en nombres entiers avec recours total pour modéliser le comportement spatialement explicite du feu et choisir les points de suppression d'un feu de forêt. Les décisions simplifiées de suppression prennent la forme de « nœuds de suppression » qui sont placés sur une matrice du paysage pour la prise de décision multiétape. Des scénarios météo sont utilisés pour représenter une distribution des changements probables de comportement du feu en réponse aux changements météorologiques aléatoires, modélisés en utilisant des arbres de probabilité des conditions météorologiques. Les décisions de suppression multiétapes et le comportement du feu réagissent à ces événements météorologiques et l'un à l'autre. Des contraintes de non-anticipativité assurent que les décisions de suppression tiennent compte de l'incertitude des prévisions météorologiques. L'étude de cas types pour ce modèle fournit des exemples d'interaction entre le comportement du feu et la suppression qui permet de réduire au minimum la superficie qui devrait être touchée par le feu et la suppression. [Traduit par la Rédaction]

Mots-clés : programmation stochastique multiétape, progression des feux de forêt, suppression des feux de forêt, incertitude au sujet des conditions météorologiques propices aux incendies.

Introduction

In a recent paper, we presented a deterministic mixed integer programming (MIP) model of fire growth and behavior that incorporated both the beneficial and the harmful effects of fire (Belval et al. 2015). Although that deterministic model provides insights into the spatial nature of fire growth and the interactions between fire behavior and suppression actions, it does not directly account for uncertainties commonly encountered in wildland firefighting. Uncertainty is, however, an important factor influencing wildland fire management decisions (see Martell (1982), Martell et al. (1998), and Miller and Ager (2013)). Sources of uncertainty may include the values of resources at risk, fuel treatment effectiveness, ecological responses to fire, missing or incomplete data, and fire behavior (Thompson and Calkin 2011). Uncertainty is particularly important in tactical fire suppression decisions, because it is inherent in fire weather predictions and thus in weather influences on future fire growth and behavior. In this paper, our aim is to extend the model presented in Belval et al. (2015) to address one of the critical uncertainties present in predicting future fire growth and behavior for fire suppression decision making, specifically by incorporating stochastic weather and resulting fire behavior. This new model formulation also recognizes that fire suppression actions in the early stages of firefighting can significantly affect fire growth and thus influence later fire management decisions.

Other spatial MIP models prior to Belval et al. (2015) were built to address the spatial fire growth and suppression problem. For example, Hof et al. (2000) built a deterministic MIP model to maximize the amount of time before fire reaches protected areas. Another example presented by Wei et al. (2011) determines suppression placement that minimizes the values lost due to a fire using the same fire arrival time assumptions as Hof et al. (2000). Neither of these models allow decisions to be made that account for stochastic fire growth.

Stochastic fire growth has been incorporated into a number of decision support models. For example, Gilless and Fried (1999) developed the fire behavior module for the California Fire Economics Simulator (CFES2), incorporating stochastic fire growth to support seasonal wildland fire preparedness decisions in California. Stochasticity in fire growth is introduced into the model using numerous sample fires (Gilless and Fried 1999). Each sample fire is simulated at a representative landscape location with deter-

Received 20 July 2015. Accepted 12 December 2015.

E.J. Belval and Y. Wei. Department of Forest and Rangeland Stewardship, Colorado State University, Fort Collins, CO 80523-1472, USA.
M. Bevers. USDA Forest Service, Rocky Mountain Research Station (emeritus), Fort Collins, CO 80526, USA.
Corresponding author: Erin J. Belval (email: mccowene@gmail.com).

ministic fire growth using one randomly drawn weather scenario combined with homogeneous fuel and terrain conditions. CFES2 assumes that fire grows in ellipses or circular shapes on representative landscapes and demonstrates an example of a quasispatial fire growth model.

In contrast, FSPro (Finney 2002) is an example of a spatial model designed to model stochastic fire behavior for single fires on a heterogeneous raster landscape comprised of homogeneous cells. A time series process is used to generate thousands of possible weather predictions (weather scenarios). Each fire is simulated for all weather scenarios (Finney 2002), and the results of these simulations are compiled to make probabilistic fire maps (Andrews 2007; Finney et al. 2011). These results are used in the Wildland Fire Decision Support System (WFDSS) in the United States to help fire managers integrate information about probable fire spread with factors affected by fire to inform suppression strategies (Calkin et al. 2011). Another example of a stochastic fire simulation model using a heterogeneous raster landscape was developed by Boychuk et al. (2009). They parameterized their model using stochastic rates of spread based on random draws from an exponential distribution. Alexandridis et al. (2011) also developed a stochastic fire spread model for a raster landscape; spread was based on the probabilities of fire transmission between cells. In the models developed by Boychuk et al. (2009) and Alexandridis et al. (2011), the random distributions used (i.e., spread rates and fire transmission probabilities) are affected by vegetation, wind, and topography. A third example designed for a single fire on a heterogeneous landscape is presented by Mandel et al. (2008), in which wildfire growth is modeled by coupled partial differential equations based on balance equations for energy and fuel. An ensemble Kalman filter integrates these equations with real data. The predictions used in the ensemble Kalman filter are produced using random perturbations of the results from the partial differential equations. As it becomes available, observed fire behavior is incorporated into the Kalman filter to achieve fire spread simulations even with erroneous initial ignition placement. Of these fire spread models, only the model by Alexandridis et al. (2011) evaluates suppression strategies, namely they investigate the effect of dropping water from an air tanker on a fire. None of the models suggest possible suppression strategies to managers.

Making fire management decisions with uncertain knowledge of future fire behavior and other factors is challenging. Stochastic programming (SP) provides a tool to design and evaluate fire management decisions, explicitly accounting for uncertainty associated with future events. For example, two-stage SP has been used to design seasonal initial attack resource deployment and dispatching plans that address containment of modeled fires. Haight and Fried (2007), Ntaimo et al. (2012), Lee et al. (2013), and Arrubla et al. (2014) modeled fires grouped by fire days on representative landscapes. Wei et al. (2015) modeled historical fires grouped by fire days using historical fire weather records. Fire behavior for each fire in these models is deterministic, and stochasticity is added by using representative scenarios or sample fire days. Of these models, only Wei et al. (2015) endogenously model the effects of ongoing suppression on fire growth.

Hu and Ntaimo (2009) outline a method to evaluate seasonal deployment and dispatching plans produced from a two-stage SP by exogenously simulating random fireline production and fire growth rates for a set of scenarios. Stochastic decision capability has also been incorporated directly into mathematical programming models for fire suppression. For example, Mees and Strauss (1992) modeled the probability of a fireline segment holding conditioned on the probability that a constructed fireline was a given width. The holding probability was then used in an integer programming model to determine which resources should be assigned to a predefined set of fireline segments. The model used deterministic fire behavior; flame length was assumed to be constant along each segment of fireline, and no stochastic scenarios of fire spread were constructed.

Fig. 1. An example of a weather situation in which average scenarios may not meaningfully represent stochastic scenarios.

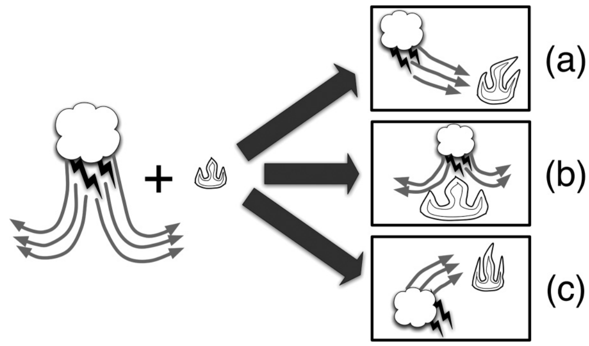

Deterministic mathematical programs do not always provide reliable, high-quality decisions in fire suppression because they do not directly address uncertainties that are typical in fire prediction and management. One deterministic approach is to examine the "mean value solution" (see Birge and Louveaux (1997)), which replaces random parameters in a stochastic model with their mean values. This, however, may oversimplify many fire spread problems. For example, average wind directions may not be meaningful. A situation that demonstrates this is shown in Fig. 1. Here, a storm cell is located west of a fire. The fire manager does not know if the storm cell will (*a*) pass north of the fire creating strong southerly drafts, (*b*) pass directly overhead, causing strong downdrafts that push the fire outward, or (*c*) pass south of the fire creating strong northerly drafts. The "average" of these three situations could be the single outward scenario, or if the cell is producing precipitation, it could be argued that the "average" here is no wind, as the northerly and southerly drafts cancel each other out.

This paper offers two main contributions to the literature on the use of SP for suppressing a given wildfire. First, we model stochastic fire growth that interacts with multistage tactical fire suppression decisions by revising and expanding the deterministic MIP model previously developed by Belval et al. (2015) to now incorporate multiple weather scenarios. Second, we introduce flexible modeling for the timing of suppression decisions either driven by weather changes or occurring at fixed times during large fire operations. This SP model allows full recourse multistage decisions (see Birge and Louveaux (1997)) using a probability distribution of weather forecasts to drive suppression placement decisions on a heterogeneous raster landscape. Suppression nodes similar to the control locations in Belval et al. (2015) are employed as a simplified form of fire suppression to test the interactions between fire spread and suppression actions. Nonanticipativity (Birge and Louveaux 1997) is enforced to reflect that suppression decisions are implemented before weather uncertainty is resolved. Test cases demonstrate solutions that minimize the expected area impacted by fire and suppression activities.

Methods

In this section, we describe the formulation of our multistage stochastic MIP model with full recourse for a fire growth and suppression problem. We optimize suppression placement decisions and resulting interdependent fire behavior using stochastic scenarios defined by probabilistic weather predictions.

Weather trees and multistage decision trees

This model requires a set of probabilistic weather predictions that are structured as a stochastic "weather tree". Three examples of such trees are shown in Fig. 2. We will refer to branches on the tree as weather "subscenarios". A new subscenario is formed each time the weather is predicted to change. A sequence of subsce-

Fig. 2. (*a*) A multistage decision tree with fixed-time decision points that correspond to weather changes. (*b*) A multistage decision tree with fixed-time decision points. (*c*) The same decision tree as (*b*) with variable-time decision points at weather changing events. The multistage decision tree in (*a*) is used to parameterize the test cases shown in Figs. 5–8, the multistage decision tree in (*b*) is used to parameterize the test case in Fig. 9, and the multistage decision tree in (*c*) is used to parameterize the test case in Fig. 10.

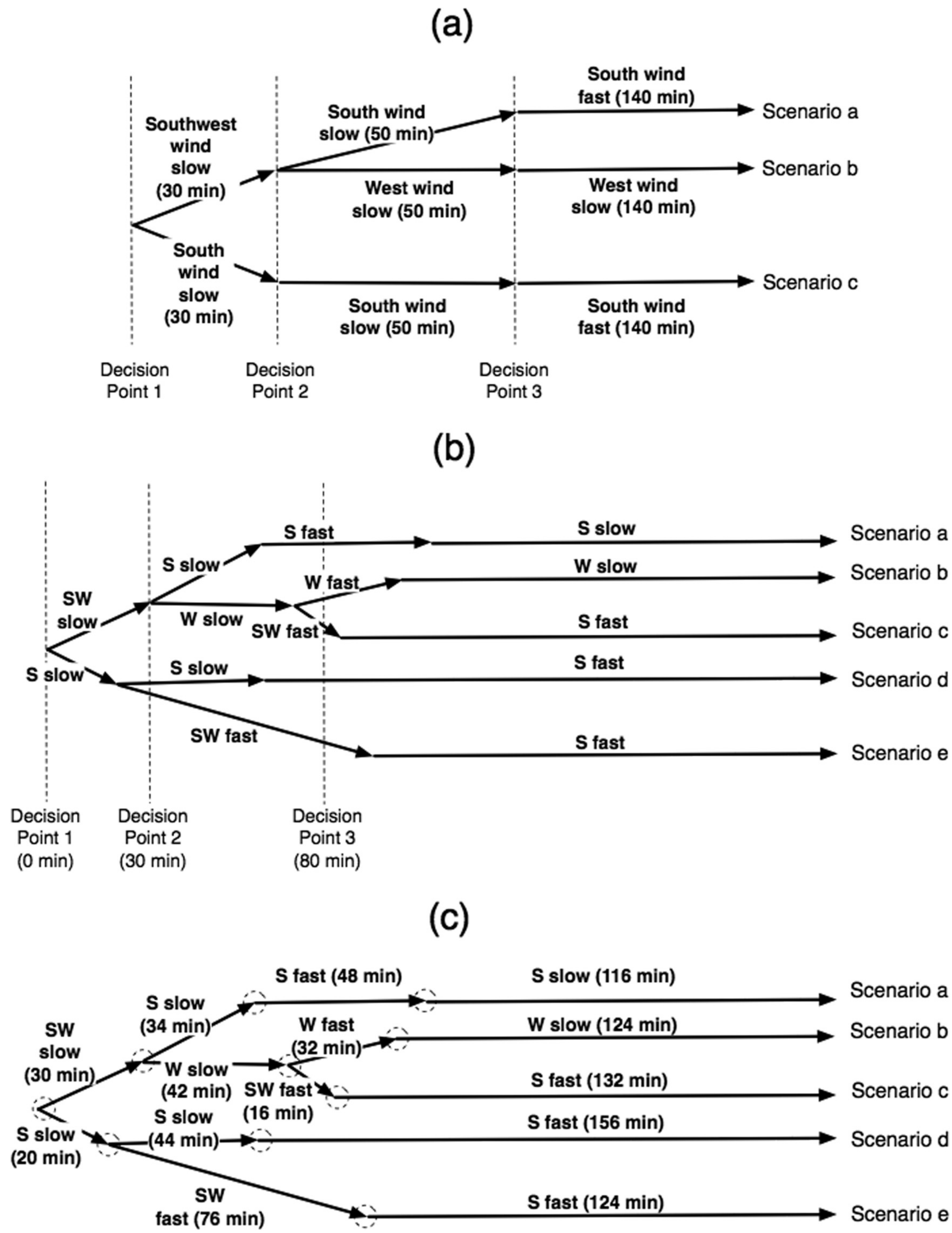

narios over time forms a weather stream, which will be referred to as a weather "scenario". The weather tree reflects uncertainty about when and how the weather may change. Each weather scenario covers the suppression planning horizon for a modeled fire event.

When decision stages are imposed on a weather tree, we refer to that tree as a "multistage decision tree". First-stage decisions determine where initial fire suppression activities should be placed. Recourse decisions determine where suppression should be placed at later stages; these recourse decisions are conditioned on the weather and suppression-driven outcomes of the preceding stages. All suppression placement decisions are selected by our model simultaneously. Suppression node placements are implemented at the beginning of each stage, which we refer to as "de-

Fig. 3. The node associated with each raster cell is assumed to be connected to the nodes of adjacent cells with which it shares an edge or vertex. This image shows an example using square raster cells (as used in testing this model).

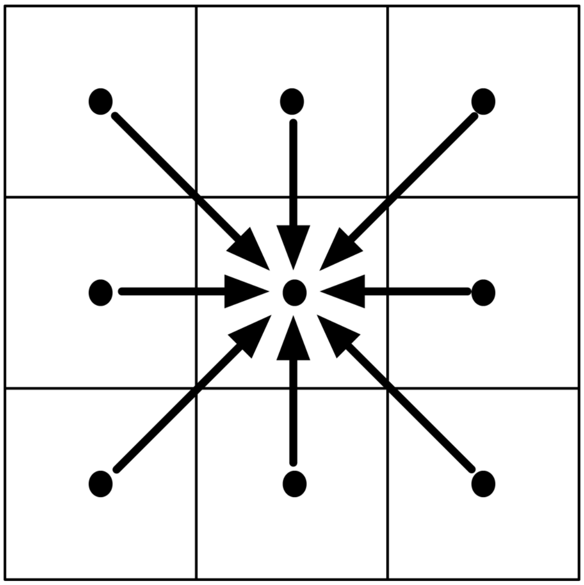

cision points". If a stage begins during a weather subscenario, then that subscenario is broken into two shorter subscenarios with identical weather parameters; one subscenario is in the stage prior to the decision point and the other subscenario is in the stage after the decision point. Decisions can be implemented at "fixed-time" decision points, which take place at consistent times across all scenarios, or at "variable-time" decision points, which take place at weather changing events. Fixed-time decision points may or may not coincide with weather changes. When all weather changes coincide with fixed-time decision points, our multistage decision tree is structured like traditional stochastic decision trees (Birge and Louveaux 1997), as shown in Fig. 2*a*. Figure 2*b* instead shows a more complex multistage decision tree where weather changes do not always coincide with fixed-time decision points. The tree in Fig. 2*c* shows weather changes identical to the tree in Fig. 2*b*. In Fig. 2*c*, however, we employ variable-time decision points at weather changing events (the circled points). We discuss the implications of these alternative structures for decision timing further in the Suppression decisions and the Discussion sections.

Spatial representation

We model fire spread and suppression on a raster landscape of square cells. Each cell represents a parcel of land modeled as having homogeneous terrain and fuel type. Over the time frame of an individual wildfire, terrain and fuel type for each cell are treated as static constants. Nodes are defined as points placed at the center of each cell. We will refer to "nodes" when discussing properties assigned to the center of the cell (e.g., fire arrival times) and to "cells" when discussing landscape properties that apply to the whole cell (e.g., fuels and terrain). We will refer to "fire spread paths" when discussing the links between neighboring nodes that allow fire to spread between them. The "binding fire spread path" is the single fire spread path that provides the earliest possible fire arrival time at each node; the fire arrival time constraint associated with this path is always active in the optimal solution of the mathematical programming model (see Hof et al. (2000) and Wei et al. (2011)). Figure 3 shows a set of nine cells and their corresponding nodes, along with the set of fire spread paths into the center node.

Model structure

This mixed integer SP model is based on the deterministic MIP model presented in Belval et al. (2015). Because the deterministic model is a single-stage model with no changes in weather, significant enhancements were required to accommodate multistage decisions and stochastic weather changes. In the stochastic model, fire spread and suppression variables need to be defined for each decision stage within each weather subscenario. Because fire may take more than one stage or subscenario to spread between neighboring nodes, new decision variables were added to track the amount of time and distance fire might spread between nodes in each subscenario. Fire arrival time and fireline intensity variables were also redesigned to accommodate multiple weather scenarios. The complete formulation of our SP model is presented in the appendix. The constraints that govern the fire spread variables are described below.

- The spatial relationship constraints require each node to be ignited exactly once by fire spreading from a neighboring node along a binding spread path. Exceptions are nodes with exogenous ignitions, nodes where suppression is placed, and nonflammable nodes. Nodes are considered to be burned exactly at the time of fire arrival; the spatial relationship constraints track which nodes burn during each stage within each subscenario and their corresponding binding fire spread paths.
- The new fire spread constraints track the amount of time that fire may be spreading between nodes in each stage within each subscenario. There are three possible situations for the spread time from one node (e.g., node A) into another node (e.g., node B) in each subscenario: (*i*) fire may not have reached node A by the end of the subscenario and thus the amount of time fire can spread from node A to node B during that subscenario is zero, (*ii*) fire may reach node A sometime during the subscenario and thus the amount of time fire can spread from node A to node B during that subscenario is the remainder of the duration of the subscenario, and (*iii*) fire may have reached node A before the beginning of the subscenario and thus the amount of time fire can spread from node A to node B during that subscenario is the entire subscenario. The distance that the fire could spread along the path from node A to node B is dependent on the fire travel time and is calculated by the fire spread constraints.
- The fire arrival time constraints rely on the fire spread constraints to determine the time and subscenario fire arrived at each node.
- Fireline intensity constraints use the binding spread path and subscenario that fire arrived at each node to calculate the corresponding fireline intensity given the weather during that subscenario.
- Fire suppression constraints limit the number of suppression nodes that can be implemented for each stage within each subscenario. They also ensure nonanticipativity; the constraints that model nonanticipative suppression decisions are explained in more detail in the Suppression decisions section below.

The new decision variables and constraints described above allow dynamic modeling of fire behavior and suppression; fire suppression in early stages influences fire behavior, which, in turn, drives fire suppression decisions in later stages. In addition, these decision variables and constraints are structured differently from many SP models (Birge and Louveaux 1997) by allowing weather changing events to differ from decision points.

For the test cases presented in this paper, we chose to use an objective function to minimize the total expected area impacted by fire and suppression activity. However, alternative objective functions could also be used. For example, Belval et al. (2015) demonstrates an objective function that incorporates beneficial effects of fire; the adaption of that objective function and many others to this SP model is straightforward.

Table 1. The notation used for the indices, sets, and parameters in the mathematical formation of the stochastic fire spread model.

Notation	Definition
Indices	
i	Index for a node of interest
j	Index for a node that potentially can spread fire directly to node i ($j \in \Omega_i$, defined below)
q	Index for a weather scenario of interest
m	Index for the stages that comprise weather scenario q
p	Index for the subscenarios that comprise stage m of weather scenario q
q_m	Index for stage m from scenario q
$q_{m,p}$	Index for subscenario p in stage m from scenario q
$q_{(m,p)-1}$	Index for the subscenario that immediately precedes sub scenario p in stage m from scenario q
Sets	
Ω_i	Set of all nodes that potentially can spread fire directly to node i. In this study, Ω_i is the set of nodes adjacent to node i as shown in Fig. 1.
Φ_q	Set of all stages that comprise weather scenario q
Ψ_{q_m}	Set of all subscenarios that comprise stage m from weather scenario q
Parameters	
n_i	Number of nodes adjacent to node i (number of elements in Ω_i)
ξ_i	Binary indicator: $\xi_i = 1$ indicates node i is nonflammable
$\varsigma_{i,q_{m,p}}$	Binary indicator: $\varsigma_{i,q_{m,p}} = 1$ indicates that an exogenously defined ignition occurs at node i in subscenario $q_{m,p}$
$f_{i,q_{m,p}}$	The ignition time corresponding to $\varsigma_{i,q_{m,p}} = 1$
$\kappa_{i,q_{m,p}}$	The fireline intensity corresponding to $\varsigma_{i,q_{m,p}} = 1$
$\kappa_{j,i,q_{m,p}}$	The fireline intensity at node i if the binding fire spread path into node i is from node j and fire arrives at node i during subscenario $q_{m,p}$
$s_{j,i,q_{m,p}}$	The rate at which fire spread from node j to node i in subscenario $q_{m,p}$
$d_{j,i}$	The distance between node j and node i
$t_{q_{m,p}}$	The length of time subscenario $q_{m,p}$ lasts
c_{q_m}	The number of suppression nodes that may be placed on the landscape at stage m in scenario q
Pr[q]	The probability of scenario q occurring
M	A large number used in the logic constraints ("big M")

Note: In this paper, lowercase Arabic and Greek letters indicate parameters, and capital Greek letters represent sets. An exception to this is "big M", which is commonly used in if–then logic constraints.

Table 2. The notation used for the response and decision variables in the mathematical formation of the stochastic fire spread model.

Notation	Definition
$D_{i,q_{m,p}}$	Binary indicator: $D_{i,q_{m,p}} = 1$ indicates that fire first arrived at node i during subscenario $q_{m,p}$
$B_{j,i,q_{m,p}}$	Binary indicator: $B_{j,i,q_{m,p}} = 1$ indicates that the binding fire spread path (earliest arrival) in scenario q for node i was from node j arriving at node i during subscenario $q_{m,p}$
$F_{i,q}$	Fire arrival time at node i for scenario q
$I_{i,q}$	Fireline intensity at node i for scenario q
$T_{j,q_{m,p}}$	Time fire could travel from node j into its neighboring nodes during subscenario $q_{m,p}$
$\mathrm{TT}_{j,q_{m,p}}$	Total time elapsed from the moment the fire first arrived at node j through the end of sub scenario $q_{m,p}$
$L_{j,i,q_{m,p}}$	Potential distance fire traveled from node j to node i during subscenario $q_{m,p}$
$\mathrm{TL}_{j,i,q_{m,p}}$	Total potential distance fire traveled from node j to node i from the moment the fire first arrived at node j through the end of subscenario $q_{m,p}$
$A_{j,i,q_{m,p}}$	Binary indicator: $A_{j,i,q_{m,p}} = 1$ indicates that for scenario q, the total distance fire traveled from node j to node i first exceeded the distance between those nodes during sub scenario $q_{m,p}$
Y_{i,q_m}	Binary indicator: $Y_{i,q_m} = 1$ indicates that suppression was placed at node i at the beginning of stage m in scenario q

Note: In this paper, capital Arabic letters are used to represent decision and response variables. All decision and response variables have an implicit lower bound of zero.

Suppression decisions

Nonanticipative decision making (Birge and Louveaux 1997) assumes that at a decision point the manager cannot anticipate exactly which weather scenario will happen and thus must account for a probability distribution of possible future scenarios. Nonanticipativity can be modeled explicitly or implicitly depending on the structure of the multistage decision tree. Examples of both are shown in Fig. 2. For an example of explicit nonanticipativity, suppose we remove scenario c from the tree in Fig. 2*a* and consider scenarios a and b as a complete tree. A weather changing event at the start of the second stage creates two branches in the tree with the branching occurring exactly at decision point 2. Two sets of suppression placement variables (see Tables 1 and 2) are explicitly built in our model in the second stage, one belonging to scenario a and the other belonging to scenario b. These two sets of suppression placement variables must be explicitly constrained to be equal using eq. A23 if nonanticipativity is desired. Using cell 1 as an example, we would impose $Y_{1,a_2} = Y_{1,b_2}$, where $Y_{1,a_2} = 1$ if suppression is located in node 1 during stage 2 of scenario b. This constraint is paired with constraints on the amount of suppression allowed in those subscenarios (see eq. A22). In contrast, only one weather branch is associated with scenarios a and b at the beginning of the first stage. Thus, a single set of suppression placement variables is built to represent the first stage of these two scenarios; this implicitly constrains suppression decisions for scenarios a and b to be the same. Again using cell 1 as an example, the decision variable Y_{1,a_1} is used for the first stage of both scenario a and scenario b.

To use the explicit equality constraints described above, decisions must occur at decision points where the following decision stages are of the same length to ensure feasibility of eq. A23. Thus, eq. A23 can be used for the tree in Fig. 2*a* to constrain suppression placements for scenarios a and b in the second stage because (*i*) a branch in the weather tree coincides with decision point 2 and (*ii*) the second stage is the same length for both scenarios. Equation A23 can also be used with the tree shown in Fig. 2*a* for decision point 1 to require all three scenarios to employ the same first stage suppression nodes. Similarly, eq. A23 can be used with the tree shown in Fig. 2*b* for decision point 1 to constrain all five scenarios to employ the same first stage suppression nodes and for decision point 2 to constrain scenarios a, b, and c to employ the same second stage suppression nodes.

If decisions vary in time and coincide with branching in the weather tree, the set of explicit nonanticipativity constraints become more complex due to the variable length of the stages. For example, given the multistage decision tree in Fig. 2*c*, where decisions are implemented at weather changing events, at the second stage of scenarios a, b, and c, we would need the nonanticipativity constraints to require all suppression actions taken in stage two of scenario a to be taken also in stage two of scenarios b and c, along with allowing some additional suppression nodes in b and c that are not allowed in scenario a. This is because scenario a has a shorter second stage (34 min) than the second stage of scenarios b and c (42 min). Using cell 1 as an example again, the nonanticipativity constraint for this situation would be $Y_{1,a_2} \le Y_{1,b_2}$, which again is paired with a constraint on the amount of suppression allowed in those subscenarios (see eq. A22). A numerical example of this is presented below in the "fixed-time decision points" test case.

Fig. 4. A contour and fuel type map showing the 11 cell × 12 cell landscape described in Table 3 and used in several test cases.

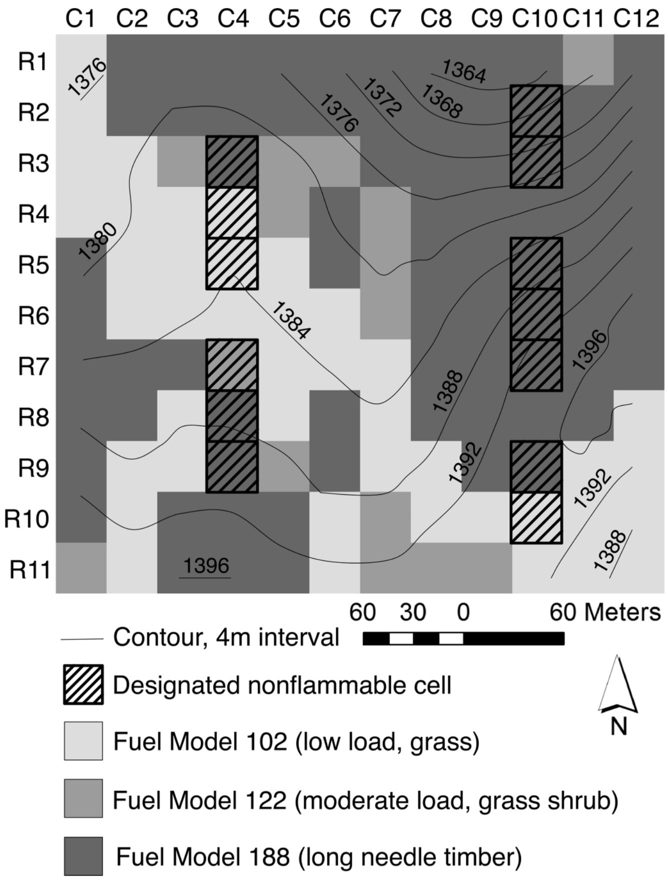

Table 3. The range of landscape values for the 11 cell × 12 cell landscape used in the test cases.

Characteristic	Value(s) used
Cell size	30 m × 30 m
Fuel model	102, 122, and 188
Elevation	1357–1397 m
Slope	0%–19%
Aspect	Generally northern
Canopy cover	Varies with fuel type
Fuel moisture (1 h, 10 h, 100 h, and live)	11%, 20%, 26%, and 100%
Southerly wind direction	180°
Southwesterly wind direction	270°
Westerly wind direction	225°
"Fast" wind speed	5.36 m·s^{-1}
"Slow" wind speed	3.58 m·s^{-1}

Test cases

The test cases presented here use an 11 cell × 12 cell heterogeneous landscape (see Fig. 4) modeled from a location in the Black Hills of South Dakota with spatial information from Landfire (U.S. Department of Interior, U.S. Geological Survey 2013). Table 3 summarizes the range of values for the 11 cell × 12 cell heterogeneous landscape, which includes some gentle to moderate slopes and is composed of fuel models 102, a "low load, dry climate grass" fuel type where fire is carried by grass; 122, a "moderate load, dry climate grass shrub" fuel type where fire is carried by grasses and shrubs; and 188, a "long needle timber" fuel type where fire is carried mainly by needle litter (Scott and Burgan 2005). All landscape boundaries are assumed to be nonflammable.

We assume that ignitions take place and initial suppression decisions are made at time $t_0 = 0$. Recourse suppression decisions are assumed to be made at fixed-time decision points of 30 min after ignition and 80 min after ignition for the runs using the multistage decision trees shown in Figs. 2*a* and 2*b*. For the test case using the multistage decision tree shown in Fig. 2*c*, recourse decisions take place at variable-time decision points, specifically, at each weather changing event. The multistage decision tree shown in Fig. 2*a* consists of three unique weather scenarios, each containing three subscenarios, to reflect combinations of wind directions (south, west, and southwest) and wind speeds ("slow", 3.58 m·s^{-1}; "fast", 5.36 m·s^{-1}) selected arbitrarily for testing purposes. This multistage decision tree is used to parameterize the results in Figs. 5–8. Figures 2*b* and 2*c* present more complex multistage decision trees based on identical weather trees but using different decision points. Figure 2*b* incorporates fixed-time recourse decision points into the multistage decision tree creating five scenarios, each with three decision stages. Figure 2*c* consists of five scenarios with variable-time recourse decisions at each weather changing event. For the weather in both Figs. 2*b* and 2*c*, combinations of wind directions (south, west, and southwest) and wind speeds ("slow", 3.58 m·s^{-1}; "fast", 5.36 m·s^{-1}) were again used. The results in Figs. 9 and 10 were parameterized using the multistage decision trees shown in Figs. 2*b* and 2*c*, respectively. We used the method described in Wei et al. (2011) and Belval et al. (2015) to calculate fire spread rates for every cell based on Rothermel's equation (Rothermel 1972).

Our first test case examines fire behavior without allowing any fire suppression using the simpler multistage decision tree shown in Fig. 2*a*; we will refer to this as the "no suppression" test case. This case tests our implementation of stochastic fire behavior and provides a point of comparison for three additional test cases that also use the multistage decision tree from Fig. 2*a*. These additional test cases allow three suppression nodes to be completed in the first stage, six nodes to be completed in the second stage, and any number of nodes to be completed in the third stage. We chose not to constrain the number of suppression nodes in the final stage to ensure that test cases contained the modeled fire. Of these three test cases, we first discuss a model run that includes nonanticipativity constraints to examine how fire suppression node placements change in the presence of uncertain future fire behavior; we will refer to this as the "nonanticipative suppression" test case. We then discuss the results from a second case where we model each scenario deterministically (the "deterministic" test case). We use these results to calculate the expected value of perfect information as suggested by Birge and Louveaux (1997). We then examine a third case where no recourse decisions are allowed; this forces identical decisions to be made across all scenarios at the start of the problem (the "no recourse" test case).

Finally, we examine results from the more complex multistage decision trees shown in Fig. 2*b* (the "fixed-time decision points" test case) and Fig. 2*c* (the "variable-time decision points" test case). For the fixed-time decision points test case, we assumed that three nodes of suppression could be completed in the first decision stage, six nodes of suppression could be completed in the second decision stage, and an unlimited number of suppression nodes could be completed in the last decision stage. Nonanticipativity was enforced for each decision stage, requiring the same nodes of suppression to be selected for all scenarios in stage one and again for scenarios a, b, and c in stage two. For the variable-time decision points case, we scaled the number of suppression nodes that could be completed to the length of the stage using eq. A22. Thus, for scenario a, three nodes of suppression could be completed in the first stage, four nodes could be completed in the second stage, six nodes could be completed in the third stage, and unlimited nodes could be completed in the final stage. Similarly, for scenarios b, c, d, and e, three, three, two, and two nodes could be completed in the first stage, respectively, five, five, five, and seven nodes could be completed in the second stage, respectively, and

Fig. 5. Fire arrival times (1) and fire spread paths and fireline intensities (2) for the 11 cell × 12 cell landscape shown in Fig. 4 for weather scenarios a, b, and c from Fig. 2*a*. No suppression nodes were placed on the landscape. The total expected number of nodes impacted in this test case is $E[Z]$ = 119.

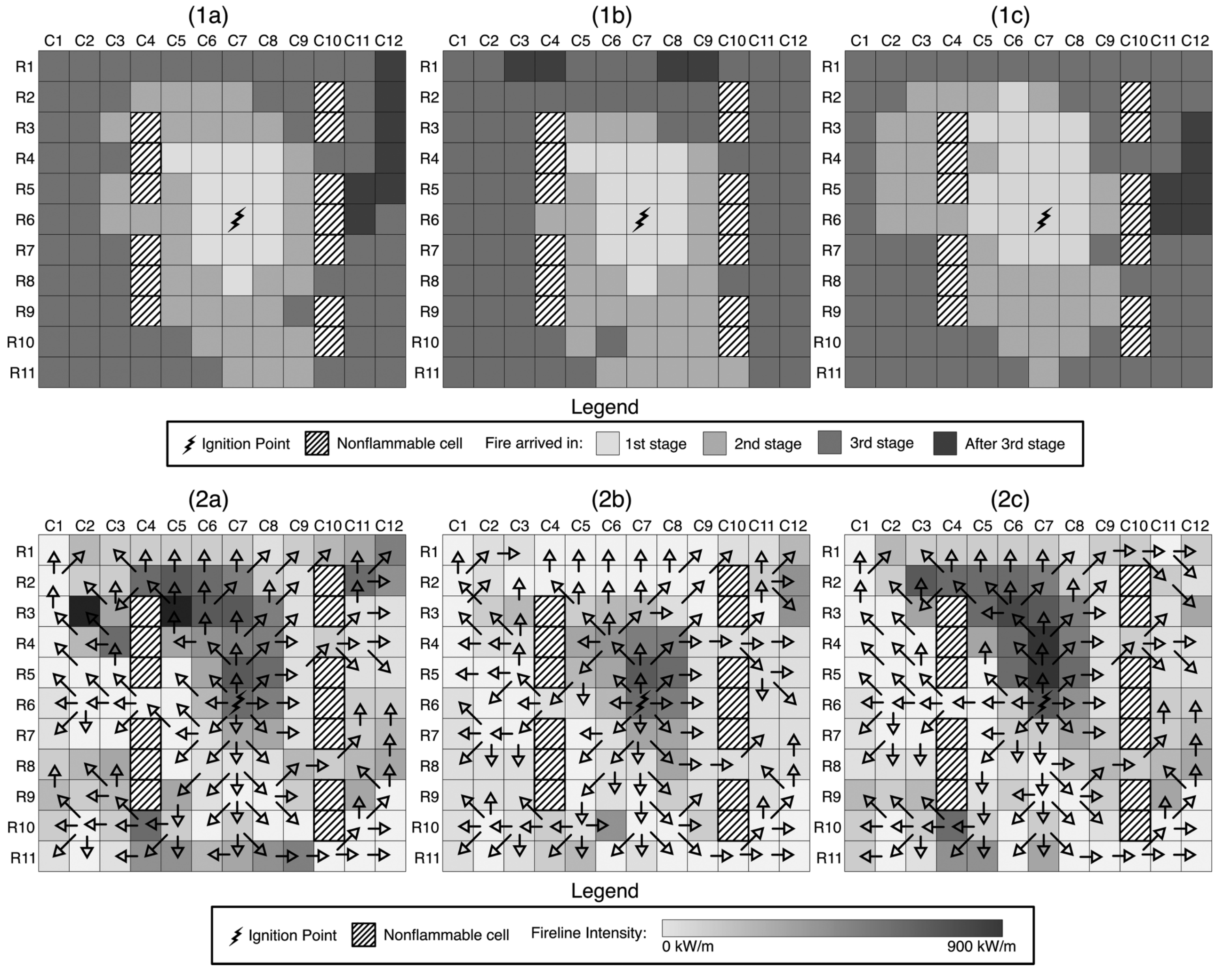

Fig. 6. Fire arrival times and suppression node locations for the 11 cell × 12 cell landscape shown in Fig. 4 for weather scenarios a, b, and c from Fig. 2*a* optimized with nonanticipative suppression. Three suppression nodes could be completed in the first stage and six suppression nodes could be completed in the second stage, with no limit for those completed in the third stage. The total expected number of nodes impacted in this test case is $E[Z]$ = 27.67.

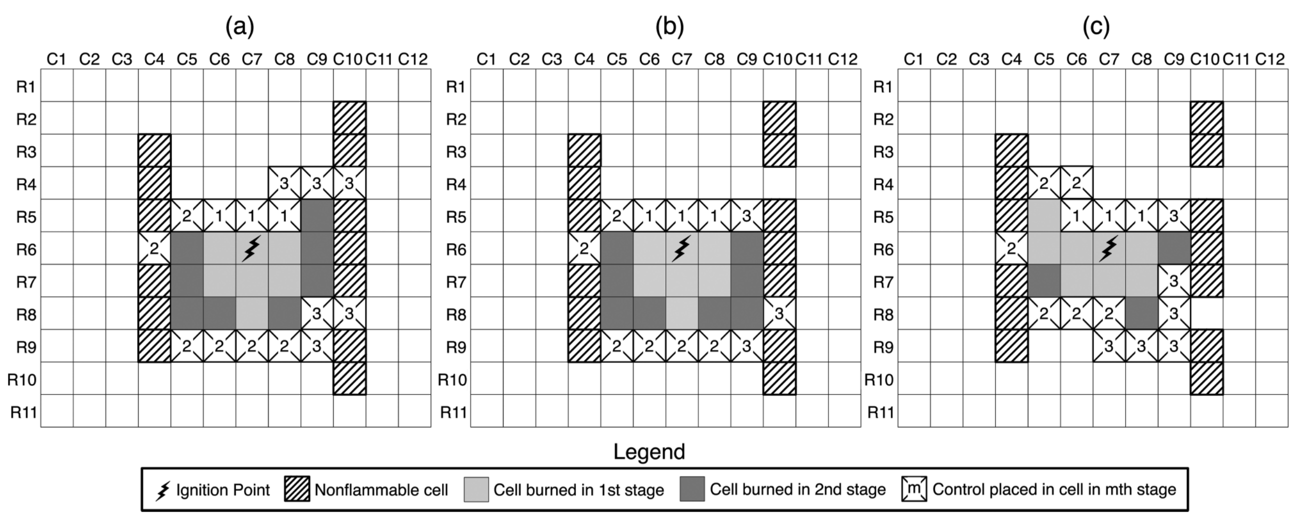

Fig. 7. Fire arrival times and suppression node locations for the 11 cell × 12 cell landscape shown in Fig. 4 for weather scenarios a, b, and c from Fig. 2*a* optimized with deterministic suppression. Three suppression nodes could be completed in the first stage and six suppression nodes could be completed in the second stage, with no limit on those completed in the third stage. The total expected number of nodes impacted in this test case is $E[Z] = 26.00$.

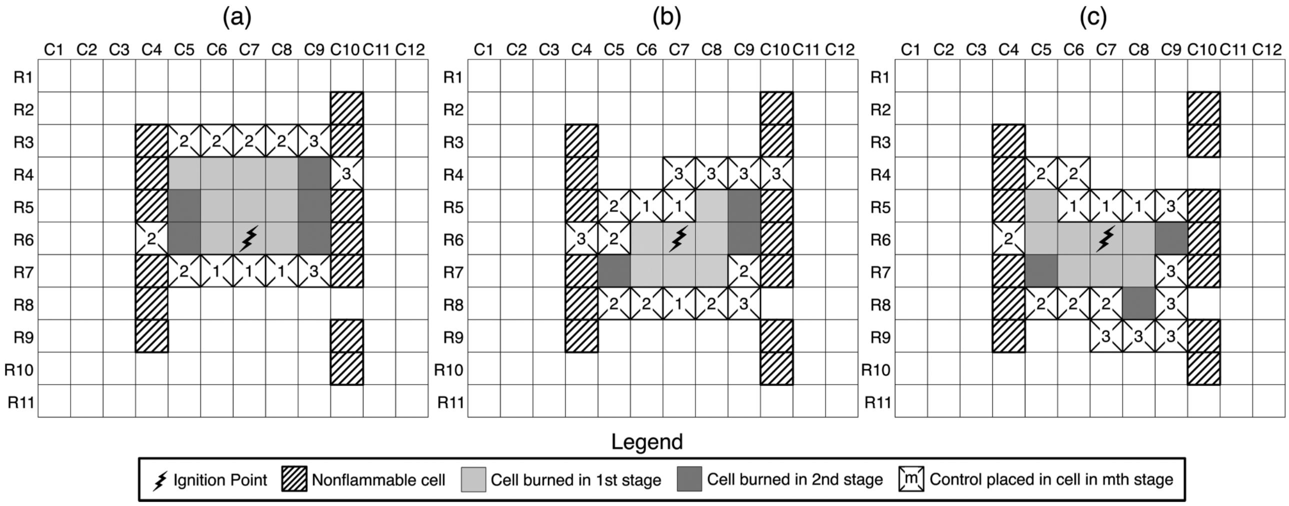

Fig. 8. Fire arrival times and suppression node locations for the 11 cell × 12 cell landscape shown in Fig. 4 for weather scenarios a, b, and c from Fig. 2*a* optimized with nonanticipative suppression without recourse. Three suppression nodes could be completed in the first stage and six suppression nodes could be completed in the second stage, with no limit on those completed in the third stage. The total expected number of nodes impacted in this test case is $E[Z] = 29.00$.

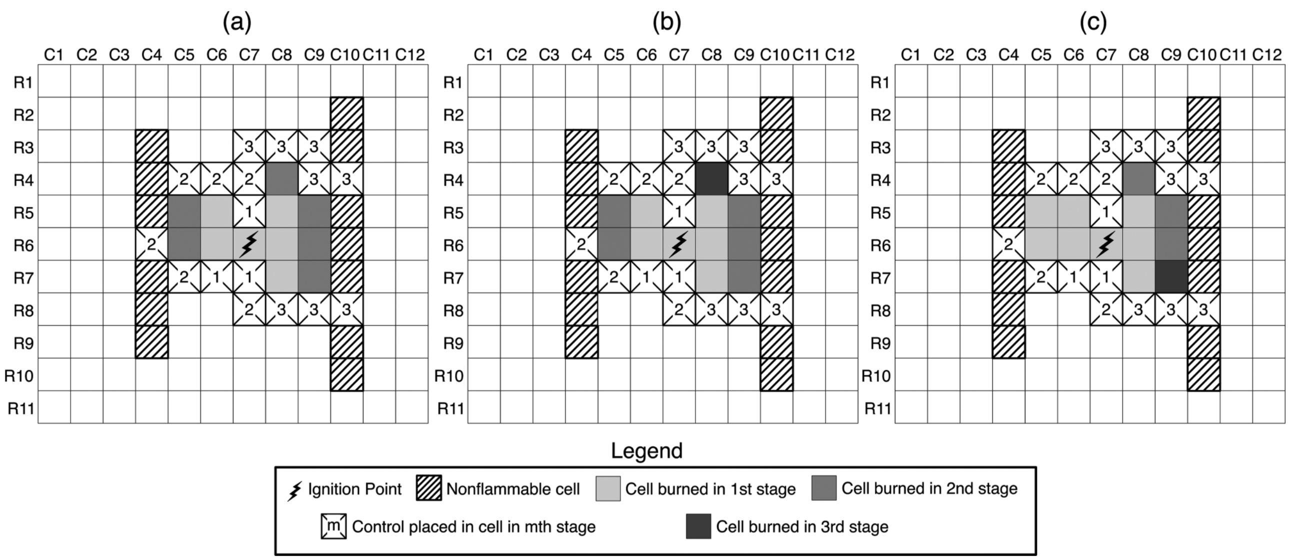

four, two, unlimited, and unlimited nodes could be completed in the third stage, respectively. Unlimited nodes could be completed for scenarios b and c in the fourth stage, and there is no fourth stage for scenarios d and e. Explicit nonanticipativity was enforced for two nodes of suppression at the first stage for all scenarios, for four nodes of suppression at the second stage of scenarios a, b, and c, for five nodes of suppression in the second stage of scenarios d and e, and for two nodes of suppression in the third stage of scenarios b and c. In all test cases, we used the objective function presented in eq. A24, minimizing the expected total area burned or impacted by suppression.

For the results using the multistage decision tree from Fig. 2*a*, we assume that the probability of each scenario is equal (i.e., $\Pr[q] = 1/3,\ \forall q$). Both the fixed-time decision points test case and the variable-time decision points test case assumed that all scenarios were equally probable (i.e., $\Pr[q] = 1/5,\ \forall q$).

Results

All figures demonstrating results use the convention that north is the top of the map. For all maps, columns a, b, and c (and d and e, if they exist) correspond to the predicted weather scenarios shown in Fig. 2. For the no suppression test case, each weather scenario is shown using two maps: one map shows the stage in which fire arrived at each node and one map shows fireline intensities and fire spread paths. For all the other test cases, which include fire suppression node placements, only one map is shown per weather scenario, indicating which nodes burned and the placement of the suppression nodes on the landscape.

Fire behavior without suppression

Without suppression, fire spreads freely across the landscape, shown here by the no suppression test case (Fig. 5). Because all cells are burned, the expected number of cells impacted for this

Fig. 9. Fire arrival times and suppression node locations for the 11 cell × 12 cell landscape shown in Fig. 4 for weather scenarios a, b, c, d, and e from Fig. 2*b* optimized with nonanticipative suppression enforced at each fixed-time decision point. The total expected number of nodes impacted in this test case is $E[Z]$ = 28.20.

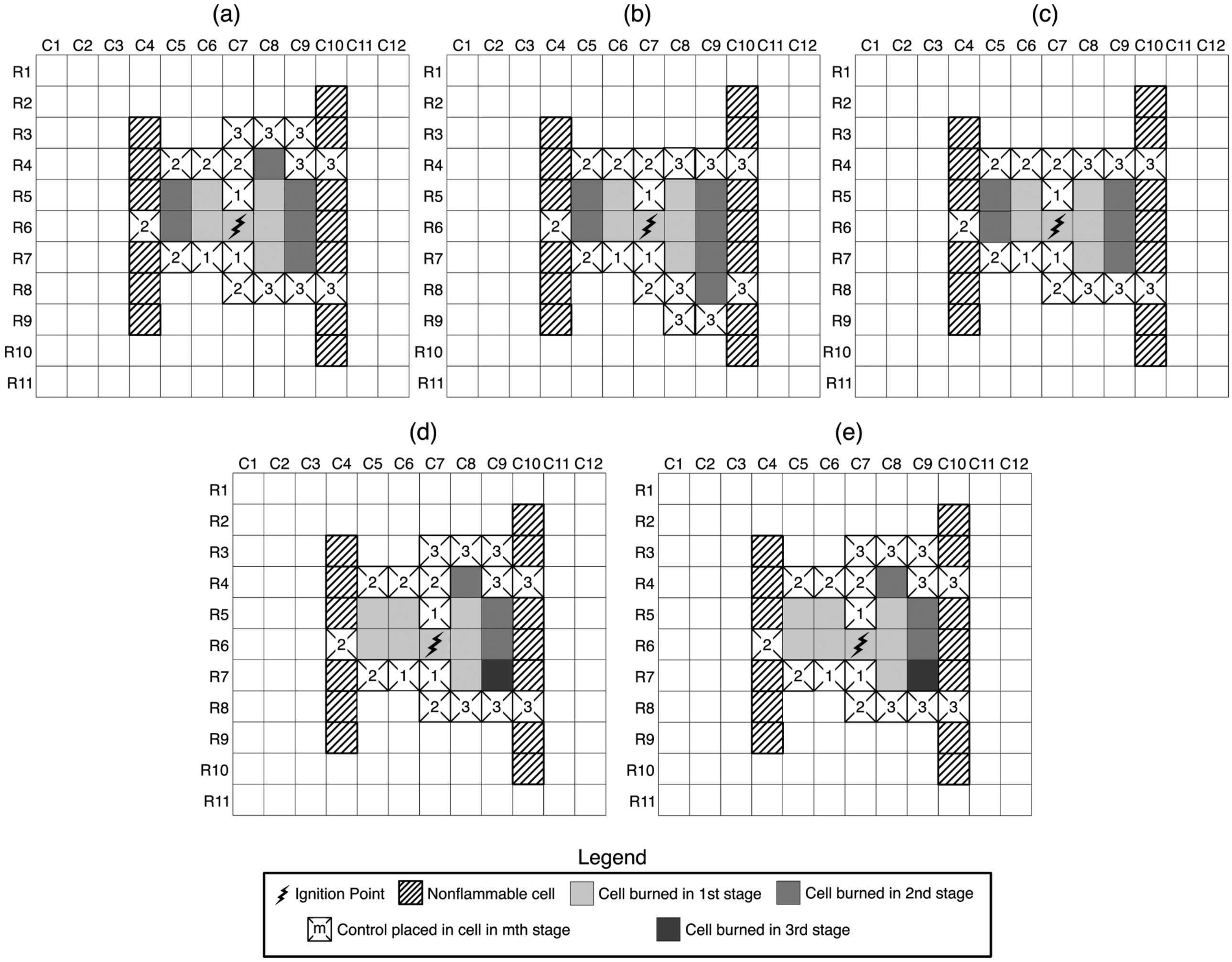

test case is the total number of burnable cells on the landscape ($E[Z]$ = 119). The first two stages of scenarios a and b (Fig. 2*a*) demonstrate how fire responds in this model to weather changes. The same weather occurs during the first stage of scenarios a and b, and thus, the model predicts the same fire behavior for the first 30 min for those scenarios. Weather forecasts diverge after 30 min, leading to different predictions of fire behavior during the following stages. This can be observed by comparing Fig. 5.1*a* with Fig. 5.1*b* and Fig. 5.2*a* with Fig. 5.2*b*. Figures 5.1*a* and 5.1*b* show that the fire arrival time at each cell for the first stage is the same; Figs. 5.2*a* and 5.2*b* show the fire spread paths and fireline intensities in the first stage are also the same. For example, fire follows the same spread path from node (C6, R4) to node (C5, R4) for both weather scenarios. In the second stage, the fire behavior differs. For example, fire spreads to nodes (C4–C7, R2) in the second stage of weather scenario a but does not spread to those nodes until the third stage in weather scenario b. The fire spread paths also vary. For example, fire spreads from node (C6, R3) to node (C7, R2) in weather scenario a but spreads from node (C7, R3) to node (C7, R2) in weather scenario b. Scenario c differs from scenario a and b in the first stage, reflecting uncertainty present within the weather predictions for the first 30 min of fire growth. An example of fire behavior during the first stage that differs between predicted scenarios is the spread path to node (C5, R4). In weather scenarios a and b, fire reaches node (C5, R4) from node (C6, R4), but in weather scenario c, fire travels from node (C5, R5) to node (C5, R4). For all nodes where fire spread paths differ by weather scenario, the fireline intensity is correspondingly altered. For example, the fireline intensities for node (C5, R3) and the fire spread paths to this node are unique for all three weather scenarios (Figs. 5.2*a*–5.2*c*).

Fire behavior interacting with nonanticipative suppression

We enforced nonanticipativity for the suppression decisions shown in Fig. 6. The first-stage decisions regarding suppression node placement are identical across all three scenarios, and the second-stage decisions are identical for scenarios a and b. In these results, 15, 15, and 11 nodes burn while using 15, 12, and 15 nodes of suppression in weather scenarios a, b, and c, respectively. This results in the total expected number of cells impacted of $E[Z]$ = 27.67.

The nonanticipative test case (Fig. 6) also demonstrates some of the benefits of modeling fire behavior and suppression nodes that respond dynamically. For example, in both weather scenarios b and c, suppression is placed at node (C9, R5) in the third stage. Figures 5.1*b* and 5.1*c* show fire arriving at this node in the second stage, so it would seem as though suppression cannot be placed at that node during the third stage. However, Figs. 5.2*b* and 5.2*c* show that without suppression, the fastest fire spread path into node (C9, R5) is from node (C8, R5). Because suppression was placed in node (C8, R5) in the first stage of the results shown in Figs. 6*b* and

Fig. 10. Fire arrival times and suppression node locations for the 11 cell × 12 cell landscape shown in Fig. 4 for weather scenarios a, b, c, d, and e from Fig. 2*c* optimized with nonanticipative suppression enforced at each variable-time decision point. The total expected number of nodes impacted in this test case is $E[Z] = 29.00$.

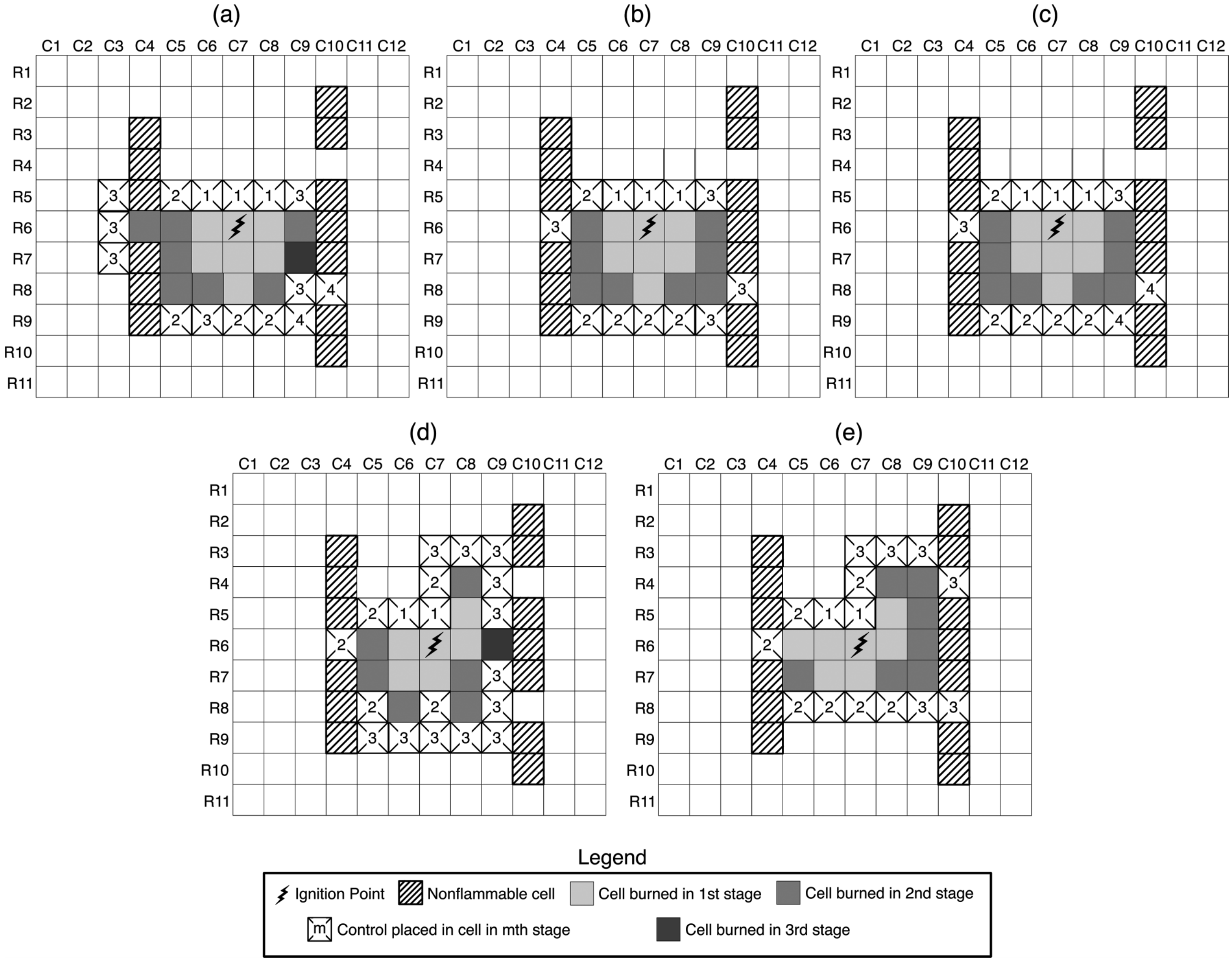

6*c*, the spread path into node (C9, R5) is altered, and the new path is slow enough that fire does not arrive until after the beginning of the third stage, allowing the suppression node placement to be delayed until the third stage.

Fire behavior interacting with deterministic suppression

Nonanticipativity was removed completely for the test case shown in Fig. 7 by treating each scenario in Fig. 2*a* as a separate problem, with all solutions contributing to the expected value objective function. The decisions shown here are exactly the decisions that would be produced by running the model on each scenario separately. For this case, the optimal suppression strategy is configured for each weather scenario as though the manager knew exactly what the future weather outcome would be and could plan for it accordingly. Because the decisions are anticipative and deterministic, the suppression strategy for each scenario is unique. The optimal solution in this case is to let 12, 9, or 11 nodes burn while placing suppression in 16, 16, or 15 nodes under weather scenarios a, b, and c, respectively. The total expected number of nodes impacted is $E[Z] = 26.00$. Compared with the nonanticipative optimal solutions, this deterministic solution appears to impact an expected 1.67 fewer cells. A critical and realistic assumption in our problem, however, is that the manager does not know what the weather will be; thus the manager must make one first-stage decision that optimizes the expected outcome given all possible weather scenarios. The selected anticipative suppression placements do not always conform with this requirement. For example, in scenario c, suppression is placed in node (C9, R7) in the third stage. In scenario b, however, fire arrives at that node in the second stage, so in the case that scenario b occurred, suppression must be placed in the second stage or earlier. In contrast, the explicit nonanticipativity constraints in our nonanticipative test case (Fig. 6) provided solutions that were feasible for all scenarios.

Fire behavior interacting with nonanticipative suppression without recourse

One strength of this multistage model is the ability to represent recourse decision making, allowing follow-up decisions to be made as new information is revealed. Without recourse decisions, identical suppression node placements must be selected for all weather scenarios. The result of restricting the model such that there are no recourse decisions is shown in Fig. 8. The total expected number of nodes impacted is $E[Z] = 29.00$. Compared with the nonanticipative decisions with recourse allowed, the difference in objective function values is the equivalent of an additional 1.33 cells impacted. One example of loss due to no recourse is node (C8, R4). In scenarios a and c, fire arrives at that node in the second stage, thus no suppression can be placed there during the third stage for any scenario. However, when recourse is allowed, suppression may be placed in node (C8, R4) in the third stage in scenario b, reducing the number of cells burned by one and eliminating two extra third-stage nodes of suppression.

Fixed-time decision points and variable-time decision points test cases

We tested identical weather trees with fixed-time decision points (Fig. 2*b*) and variable-time decision points (Fig. 2*c*) to compare two possible management styles and demonstrate how these may affect suppression node placement. Nonanticipativity is enforced in both test cases. The results from using fixed-time decision points are shown in Fig. 9, and the results from using variable-time decision points are shown in Fig. 10. Because the weather patterns used were identical, the differences in choice of suppression nodes and objective function values are only due to changes in decision timing. The total expected number of nodes impacted in the fixed-time decision points test case is $E[Z] = 28.20$ and in the variable-time decision points test case is $E[Z] = 29.00$.

Given fixed-time decision points, the three suppression nodes chosen for the first stage were (C7, R5), (C6, R7), and (C7, R7). For the variable-time decision points, the two suppression nodes chosen for the first stage were (C6, R5) and (C7, R5). In scenarios a, b, and c, a third node (C8, R5) is allowed in the first stage; in scenarios d and e, this third suppression node is not allowed until the second stage starts because of the shorter duration of the first stage. Therefore, for the variable-time decision points case, the final patterns of area affected are similar for scenarios a, b, and c but differ noticeably for scenarios d and e. With fixed-time decision points, the final patterns of area affected are similar across all scenarios in our results.

Solution times and algorithm issues

All solution times given are from an HP xw8600 Workstation with 32 GB of available RAM running Windows Vista. We initially ran CPLEX version 12.6 (IBM 2013) interactively using the default settings. We found that the solution algorithms using the default settings did not keep the fire arrival time equations (eqs. A17 and A18) feasible for the nodes on the outer edges of the landscape. The initial run we did for the no-suppression case using Fig. 2*a* returned a solution that, on close examination, was infeasible because some of the fire spread paths were incorrect. Tightening the simplex feasibility tolerance from the default 1×10^{-6} to the smallest allowed value of 1×10^{-9} solved this problem. Our results required less than a minute of solution time using the updated settings for the test case with no suppression. The results for the deterministic suppression test case took about 1 h to solve and the test cases with nonanticipative suppression took just under 0.5 h to solve. The more complex multistage decision trees (Figs. 2*b* and 2*c*) took substantially more time to solve, i.e., several hours for both test cases.

We also attempted to implement the beneficial effects of fire into this model (adapted from Belval et al. (2015)). Although the adaption of the equations was straightforward, getting an optimal solution was not straightforward. The program ran for several days but did not reduce the MIP gap below 29% for a test case using the landscape in Fig. 4 and the multistage decision tree shown in Fig. 2*a*.

Discussion

This paper introduces a stochastic MIP model that predicts fire behavior and optimizes the placement of suppression nodes for a raster landscape given a multistage stochastic decision tree. Results showed fire behavior reacting to suppression decisions under different decision tree and anticipativity assumptions. The mathematical program explicitly models fireline intensity along different fire spread paths. The stochastic fire behavior model and integrated suppression presented in this paper are an important improvement on Belval et al. (2015), as demonstrated in our test cases. For example, the suppression decisions provided by the deterministic test case were not feasible for all weather scenarios (Fig. 7), whereas the nonanticipative suppression decisions are feasible for all weather scenarios (Fig. 6). Similarly, although the no-recourse test case did provide feasible suppression decisions for all weather scenarios (Fig. 8), the objective function value was suboptimal when compared with the nonanticipative solution with recourse decisions.

The fixed-time decision points and the variable-time decision points test cases (Figs. 9 and 10, respectively) use different assumptions regarding decision-stage timing and how many suppression nodes could be placed during each stage, leading to unique solutions. The results demonstrate the importance of considering management styles when creating our multistage decision trees. Fixed-time decision points may reflect large fire incident command team decision making, where decisions are likely to be implemented at predetermined briefing times. Variable-time decision points may better reflect initial attack decision making, where a smaller, more flexible force of firefighters can quickly identify and respond to weather changes. In reality, most managers probably use a mix of the two. This model accommodates these approaches by allowing flexible decision-point timing.

Our multistage decision trees can also be crafted to reflect cases where decisions are implemented shortly after weather changes. Such trees might more realistically reflect how firefighting forces adjust to weather changes. In Fig. 2*b*, for example, if we consider scenarios d and e as forming a complete tree, the first stage has a single weather subscenario for the first 20 min, followed by a weather changing event leading to two different possible subscenarios. A decision point can be added shortly after the weather changing event, e.g., decision point 2 shown in Fig. 2*b*. The implicit nonanticipativity in the first stage provides a single set of suppression nodes in that stage for both scenarios d and e. Firefighters can then adjust specifically to either subscenario in the second stage, upon observing which weather event occurs. Adding decision points shortly following weather changing events may allow for a better objective function value because quick adjustments can be made to the suppression strategy in response to weather changes.

Although this model is still in the development phase, with substantial enhancements it might be used for suppression training or in seasonal suppression planning and deployment models. One of the critical enhancements needed is to incorporate more realistic suppression decisions. The suppression decisions used in this model are simplistic. They are more nuanced than the suppression used by Belval et al. (2015) because the model schedules the locations of suppression nodes in specific decision stages. Our suppression nodes do not, however, account for the spatial restrictions of movements, e.g., crew travel and suppression actions often are spatially continuous. Likewise, the formulation does not address resource travel time or the time required to implement suppression. This model currently assumes that suppression nodes are implemented instantaneously at decision points; in reality, suppression only has to be in place in advance of fire arrival, taking into account the time needed to allow safe fire operations. We assume that if suppression is placed at a node, then the node becomes nonflammable. In reality, if a fireline is not robust enough, fire may jump the line. Therefore, further research to develop more realistic suppression variables and related constraints would be useful. Additional enhancements such as incorporating spot fires and re-burns into the fire spread model and adding aerial resources and burnout operations to the suppression decisions could also be important topics for future research.

Because fire management tends to be a risk averse field (Canton-Thompson et al. 2008), future research might also investigate decisions that minimize the fire damage caused by the worst case scenario or constraints that restrict the probability of fire escapes or other undesirable outcomes. Useful methods to optimize these risk averse objectives might include robust optimization and chance constrained programming (Calafiore and Dabbene 2006). In addition, recent US efforts have emphasized recognizing when fire can be beneficial. Other objective functions might be used to balance the benefits and losses from wildfires. For example, weights could be placed on cells to reflect priority protection points or areas that contain property or highly valued resources. One advantage of the model presented in this paper is that fire behavior which results from differing spread paths or weather scenarios can be identified as harmful or beneficial reflecting the tracked fireline intensities. Interested readers can find an example of a fireline intensity based objective function in the model developed by Belval et al. (2015). Because a variety of objectives might be used in fire management, examining which objective functions appropriately reflect current fire policy and management may have to be handled case by case.

The objective function also influences the computer solution times. In this study, we did not present results for test cases that incorporated both the beneficial and harmful effects of fire. Optimal solutions are difficult to find for these problems. The interactions between fire spread paths and fireline intensity may cause the multiple objective problem to be more difficult than the simpler problem of containment only.

The MIP model built in this paper is more complex than the deterministic model developed by Belval et al. (2015). Consequently, large landscapes present harder problems to solve. As our tested landscapes grew in size, the solution algorithms had a larger decision space to search, requiring more computing time. For example, several smaller prototype test cases on a 6 cell × 6 cell landscape with suppression solved within a minute. The test cases on the 11 cell × 12 cell landscape in this paper required between 1 min (for the test case without suppression) and several hours (for test cases with suppression and more complex multistage decision trees) to solve. Future work to reduce solution times might include preselecting candidate solutions to reduce the decision space and building heuristics that quickly produce near optimal solutions for larger landscapes. For example, a set of cells might be identified as not suitable for suppression and could be eliminated from the set of possible suppression nodes. Further, some cells might be identified as being practical for suppression only if other cells are also selected (such as building a continuous line), and these considerations could be added as constraints on the suppression nodes that would reduce the number of possible solutions, potentially reducing solution times.

To support the implementation of this system, work is also needed in other disciplines. For example, fire weather drives stochastic fire spread patterns and fire suppression decisions on a given landscape. Constructing sound probabilistic weather scenarios based on weather forecasting is a complex and challenging task. Accomplishing this task is critical to implementing our SP method for field application.

Our SP model selects suppression node placements that alter resulting fire behavior. Explicit nonanticipativity constraints ensure that the model produces suppression decisions that account for uncertainty in weather forecasts. Weather uncertainty is represented using probabilistic weather trees. Recourse decisions allow the model to create optimal suppression decisions for each weather scenario as new information becomes available. Flexible decision points allow a variety of management styles to be represented. This stochastic approach is a step forward in modeling fire behavior and suppression in a mathematical programming framework.

Acknowledgements

This research was supported by Joint Venture Agreement 11-JV-11221636-146 between the USDA Forest Service Rocky Mountain Research Station and Colorado State University. The authors thank the associate editor and the referees whose insightful suggestions significantly improved this paper.

References

Alexandridis, A., Russo, L., Vakalis, D., Bafas, G.V., and Siettos, C.I. 2011. Wildland fire spread modelling using cellular automata: evolution in large-scale spatially heterogeneous environments under fire suppression tactics. Int. J. Wildland Fire, **20**(5): 633–647. doi:10.1071/WF09119.

Andrews, P.L. 2007. Behaveplus fire modeling system: past, present, and future. *In* Proceedings of 7th Symposium on Fire and Forest Meteorology. American Meteorological Society.

Arrubla, J.A.G., Ntaimo, L., and Stipling, C. 2014. Wildfire initial response planning using probabilistically constrained stochastic integer programming. Int. J. Wildland Fire, **23**(6): 825–838. doi:10.1071/WF13204.

Belval, E.J., Wei, Y., and Bevers, M. 2015. A mixed integer program to model spatial wildfire behavior and suppression placement decisions. Can. J. For. Res. **45**(4): 384–393. doi:10.1139/cjfr-2014-0252.

Birge, J.R., and Louveaux, F. 1997. Introduction to stochastic programming. Springer, New York.

Boychuk, D., Braun, W.J., Kulperger, R.J., Krougly, Z.L., and Stanford, D.A. 2009. A stochastic forest fire growth model. Environ. Ecol. Stat. **16**: 133–151. doi:10.1007/s10651-007-0079-z.

Calafiore, G., and Dabbene, F. 2006. Probabilistic and randomized methods for design under uncertainty. Springer, London.

Calkin, D.E., Thompson, M.P., Finney, M.A., and Hyde, K.D. 2011. A real-time risk assessment tool supporting wildland fire decisionmaking. J. For. **109**(5): 274–280.

Canton-Thompson, J., Gebert, K.M., Thompson, B., Jones, G., Calkin, D.E., and Donovan, G. 2008. External human factors in incident management team decisionmaking and their effect on large fire suppression expenditures. J. For. **106**(8): 416–424.

Finney, M.A. 2002. Fire growth using minimum travel time methods. Can. J. For. Res. **32**(8): 1420–1424. doi:10.1139/x02-068.

Finney, M.A., Grenfell, I.C., McHugh, C.W., Seli, R.C., Trethewey, D., Stratton, R.D., and Brittain, S. 2011. A method for ensemble wildland fire simulation. Environ. Model. Assess. **16**: 153–167. doi:10.1007/s10666-010-9241-3.

Gilless, J.K., and Fried, J.S. 1999. Stochastic representation of fire behavior in a wildland fire protection planning model for California. For. Sci. **45**(4): 492–499.

Haight, R.G., and Fried, J.S. 2007. Deploying wildland fire suppression resources with a scenario-based standard response model. INFOR. **45**(1): 31–39. doi:10.3138/infor.45.1.31.

Hof, J., Omi, P.N., Bevers, M., and Laven, R.D. 2000. A timing-oriented approach to spatial allocation of fire management effort. For. Sci. **46**(3): 442–451.

Hu, X., and Ntaimo, L. 2009. Integrated simulation and optimization for wildfire containment. TOMACS. **19**(4): 1–29. doi:10.1145/1596519.1596524.

IBM 2013. IBM ILOG CPLEX Optimization Studio CPLEX. User's manual. Version 12, release 6. Available from http://www-01.ibm.com/support/knowledgecenter/SSSA5P_12.6.2/ilog.odms.studio.help/pdf/usrcplex.pdf [accessed 16 July 2015].

U.S. Department of Interior, U.S. Geological Survey. 2013. LANDFIRE data distribution site. Landscape (LCP) layer last updated June 2013. [Online]. Available from http://landfire.cr.usgs.gov/viewer/ [accessed 3 September 2014].

Lee, Y., Fried, J.S., Albers, H.J., and Haight, R.G. 2013. Deploying initial attack resources for wildfire suppression: spatial coordination, budget constraints, and capacity constraints. Can. J. For. Res. **43**(1): 56–65. doi:10.1139/cjfr-2011-0433.

Mandel, J., Bennethum, L.S., Beezley, J.D., Coen, J.L., Douglas, C.C., Kim, M., and Vodacek, A. 2008. A wildland fire model with data assimilation. Math. Comput. Simulat. **79**: 584–606. doi:10.1016/j.matcom.2008.03.015.

Martell, D.L. 1982. A review of operational research studies in forest fire management. Can. J. For. Res. **12**(2): 119–140. doi:10.1139/x82-020.

Martell, D.L., Gunn, E.A., and Weintraub, A. 1998. Forest management challenges for operational researchers. Eur. J. Oper. Res. **104**: 1–17. doi:10.1016/S0377-2217(97)00329-9.

Mees, R., and Strauss, D. 1992. Allocating resources to large wildland fires: a model with stochastic production rates. For. Sci. **38**(4): 842–853.

Miller, C., and Ager, A.A. 2013. A review of recent advances in risk analysis for wildfire management. Int. J. Wildland Fire, **22**: 1–14. doi:10.1071/WF11114.

Ntaimo, L., Arrubla, J.A.G., Stirpling, C., Young, J., and Spencer, T. 2012. A stochastic programming standard response model for wildfire initial attack planning. Can. J. For. Res. **42**(6): 987–1001. doi:10.1139/x2012-032.

Rothermel, R.C. 1972. A mathematical model for predicting fire spread in wildland fuels. USDA Forest Service, Intermountain Forest and Range Experiment Station, Ogden, Utah, Research Paper INT-115.

Scott, J.H., and Burgan, R.E. 2005. Standard fire behavior fuel models: a comprehensive set for use with Rothermel's surface fire spread models. USDA Forest Service, Rocky Mountain Research Station, Fort Collins, Colorado, General Technical Report RMRS-GTR-153.

Thompson, M.P., and Calkin, D.E. 2011. Uncertainty and risk in wildland fire management: a review. J. Environ. Manage. **92**: 1895–1909. doi:10.1016/j.jenvman.2011.03.015. PMID:21489684.

Wei, Y., Rideout, D.B., and Hall, T.B. 2011. Toward efficient management of large fires: a mixed integer programming model and two iterative approaches. For. Sci. **57**(5): 435–447.
Wei, Y., Bevers, M., and Belval, E. 2015. A chance constrained programming model to allocate wildfire initial attack resources for a fire season. For. Sci. **61**(2): 278–288. doi: 10.5849/forsci.14-112.

Appendix A

This appendix presents the mathematical formulation of the stochastic mixed integer programming model for fire behavior and suppression. For this model, we are using a discrete approximation of a continuous problem, spatially (i.e., nodes in raster cells), temporally (i.e., predefined decision points and weather changes), and by employing a discrete probability distribution (i.e., representative weather scenarios). Fire spread, distances, and arrival times, however, are continuous. We use the probabilities and outcomes of each weather scenario to solve for optimal expected values, minimizing the total expected area impacted by the fire and by fire suppression operations. An optimal solution to the mathematical program reports the set of selected suppression nodes for each stage and the resulting binding fire spread paths, along with fire arrival times and fireline intensities along all binding fire spread paths for each weather scenario. The notation used to present the model is listed in Tables 1 and 2.

Spatial relationship constraints

Equations A1–A4 define the spatial relationships between the nodes in the landscape.

$$\text{(A1)}\qquad 1 - \xi_i \geq \sum\nolimits_{m \in \Phi_q}\left(Y_{i,q_m} + \sum\nolimits_{p \in \Psi_{q_m}} D_{i,q_{m,p}}\right) \quad \forall i, q$$

$$\text{(A2)}\qquad \sum\nolimits_{m \in \Phi_q}\left(Y_{i,q_m} + \sum\nolimits_{p \in \Psi_{q_m}} D_{i,q_{m,p}}\right) + \xi_i \geq \sum\nolimits_{m \in \Phi_p}\sum\nolimits_{p \in \Psi_{q_m}}(D_{j,q_{m,p}} + s_{i,q_{m,p}}) \quad \forall i, j \in \Omega_i, q$$

$$\text{(A3)}\qquad \sum\nolimits_{j \in \Omega_i} B_{j,i,q_{m,p}} = D_{i,q_{m,p}} - s_{i,q_{m,p}} \quad \forall i, q, m \in \Phi_q,\ p \in \Psi_{q_m}$$

$$\text{(A4)}\qquad B_{j,i,q_{m,p}} \leq \sum\nolimits_{k=1}^{m}\sum\nolimits_{r=1}^{p} D_{j,q_{k,r}} \quad \forall i, j \in \Omega_i,\ q, m \in \Phi_q,\ p \in \Psi_{q_m}$$

Equation A1 allows each node i to burn only once per scenario if node i is flammable but never allows node i to burn if node i is nonflammable or if suppression has been placed at node i. Equation A2 requires node i to burn in scenario q if node i has a neighbor j that burns in scenario q or if node i was ignited during scenario q, unless suppression is placed at node i. Equation A3 enforces the condition that if node i burns and cell i did not contain an ignition then the fire must have come from some neighboring node j. Lastly, eq. A4 ensures that fire cannot spread from node j to node i unless node j has burned during or before subscenario $q_{m,p}$. These equations assume that if a node is chosen for suppression, then the suppression is effective at the beginning of the stage in which it is placed. Because each node has a fire arrival time associated with it, a node is not considered burned at the beginning or end of the scenario but, rather, exactly at the time of the first fire arrival.

If any unburned nodes exist at the end of a scenario with neighbors that have burned, then eq. A2 will be violated and the model will be infeasible. To avoid this, after the multistage decision tree is built, a terminal subscenario is added to the end of each weather scenario that lasts at least until the latest possible fire arrival time. We use $p^{\sim}$ to denote this final set of weather parameters, and the corresponding subscenario is denoted by $q_{p^{\sim}}$. The predictions of fire growth from subscenario $q_{p^{\sim}}$ are considered outside the boundary of the problem. No decision stage is associated with this subscenario, and thus, suppression actions are not considered. Note that none of the trees in Fig. 2 show these terminal subscenarios.

Potential fire spread calculation constraints

Because the planning horizon is divided into subscenarios according to weather changing events, fire may take more than the length of one subscenario to travel from a node to a neighboring node. Correspondingly, the amount of time it takes for fire to travel over each spread path may need to be calculated using more than one rate of spread parameter because the rate of spread changes with the weather. We also must calculate the distance corresponding to the travel time for use in the fire arrival time constraints.

$$\text{(A5)}\qquad T_{j,q_{m,p}} \leq M\sum\nolimits_{k=1}^{m}\sum\nolimits_{r=1}^{p} D_{j,q_{k,r}} \quad \forall j, q, m \in \Phi_q,\ p \in \Psi_{q_m}$$

$$\text{(A6)}\qquad T_{j,q_{m,p}} \leq \left(\sum\nolimits_{k=1}^{m}\sum\nolimits_{r=1}^{p} t_{k,r}\right) - F_{j,q} + M(1 - D_{j,q_{m,p}}) \quad \forall j, q, m \in \Phi_q,\ p \in \Psi_{q_m}$$

$$\text{(A7)}\qquad T_{j,q_{m,p}} \geq \left(\sum\nolimits_{k=1}^{m}\sum\nolimits_{r=1}^{p} t_{k,r}\right) - F_{j,q} - M(1 - D_{j,q_{m,p}}) \quad \forall j, q, m \in \Phi_q,\ p \in \Psi_{q_m}$$

$$\text{(A8)}\qquad T_{j,q_{m,p}} \leq t_{q_{m,p}} + M\left(1 - \sum\nolimits_{k=1}^{m-1}\sum\nolimits_{r=1}^{p} D_{j,q_{k,r}}\right) \quad \forall j, q, m \in \Phi_q | m > 1,\ p \in \Psi_{q_m}$$

$$\text{(A9)}\qquad T_{j,q_{m,p}} \geq t_{q_{m,p}} - M\left(1 - \sum\nolimits_{k=1}^{m-1}\sum\nolimits_{r=1}^{p} D_{j,q_{k,r}}\right) \quad \forall j, q, m \in \Phi_q | m > 1,\ p \in \Psi_{q_m}$$

Three situations are possible regarding the time during which fire may travel from node j into its neighbors during subscenario $q_{m,p}$ addressed by eqs. A5–A9. First, fire has not reached node j by the end of subscenario $q_{m,p}$; therefore, during subscenario $q_{m,p}$, fire cannot spend any time spreading from node j to its neighbors. Given this situation, eq. A5 is binding and sets the travel time along the fire spread paths from node j to its neighbors during subscenario $q_{m,p}$ to zero. Second, fire reaches node j during subscenario $q_{m,p}$, resulting in fire spreading along the paths from node j to its neighbors during the remainder of the subscenario. Equations A6 and A7 are binding in this situation and calculate the length of time that occurs between fire arriving at node j and the end of subscenario $q_{m,p}$. Third, fire reached node j prior to subscenario $q_{m,p}$, resulting in fire spreading along the paths from node j to its neighbors for the whole subscenario. In this situation, eqs. A8 and A9 are binding, setting the time that fire travels from node j to its neighbors to the length of subscenario $q_{m,p}$.

$$\text{(A10)}\qquad TT_{j,q_{m,p}} = \sum\nolimits_{k=1}^{m}\sum\nolimits_{r=1}^{p} T_{j,q_{k,r}} \quad \forall j, q, m \in \Phi_q,\ p \in \Psi_{q_m}$$

$$\text{(A11)}\qquad TT_{j,q_0} = 0 \quad \forall j, q$$

Equation A10 calculates the total time elapsed from the moment the fire first arrived at node j through the end of subscenario $q_{m,p}$. Equation A11 initializes the total time fire spreads from node j to its neighbors at the beginning of the first subscenario to zero.

$$\text{(A12)}\qquad L_{j,i,q_{m,p}} = s_{j,i,q_{m,p}} T_{j,q_{m,p}} \quad \forall i, j \in \Omega_i,\ q, m \in \Phi_q,\ p \in \Psi_{q_m}$$

$$\text{(A13)}\qquad \mathrm{TL}_{j,i,q_{m,p}} = \sum_{k=1}^{m}\sum_{r=1}^{p} L_{j,i,q_{k,r}} \quad \forall i,j \in \Omega_i,\ q,m \in \Phi_q,\ p \in \Psi_{q_m}$$

$$\text{(A14)}\qquad \mathrm{TL}_{j,i,q_0} = 0 \quad \forall i,j \in \Omega_i, q$$

The distance that the fire traveled from node j to node i during subscenario $q_{m,p}$ can be calculated using the length of time fire spread from node j to its neighbors during subscenario $q_{m,p}$ and the precalculated rate of spread ($s_{j,i,q_{m,p}}$) from node j to node i during subscenario $q_{m,p}$ (eq. A12). Equation A13 determines the total potential distance that fire spreads from node j to node i by the end of subscenario $q_{m,p}$, including all distance covered in previous subscenarios. At the beginning of the first subscenario (m = 1, p = 1), the fire has not traveled any distance from j to i; therefore, eq. A14 sets the initial total distance traveled from node j to node i to zero.

Fire arrival time constraints

Each node receives fire from a single binding fire spread path for each weather scenario. As discussed above, the spread paths may take more than one subscenario to complete. Equations A5–A13 inform the model of the time and corresponding distance that the fire travels along each spread path in each subscenario. The following arrival time equations use this information to determine the binding spread paths and corresponding fire arrival times for each node.

$$\text{(A15)}\qquad F_{i,q} = f_{i,q_{m,p}} \quad \forall\{i|s_{i,q_{m,p}} = 1\}$$

$$\text{(A16)}\qquad \mathrm{TL}_{j,i,q_{m,p}} \le d_{j,i} + M\left(\sum_{k=1}^{m}\left(Y_{i,q_k} + \sum_{r=1}^{p} A_{j,i,q_{k,r}}\right) + \xi_i\right) \quad \forall i,j \in \Omega_i, q, m \in \Phi_q, p \in \Psi_{q_m}$$

$$\text{(A17)}\qquad F_{i,q} \le F_{j,q} + \mathrm{TT}_{j,q_{(m,p)-1}} + \frac{d_{j,i} - \mathrm{TL}_{j,i,q_{(m,p)-1}}}{s_{j,i,q_{m,p}}} + M(1 - A_{j,i,q_{m,p}}) \quad \forall i,j \in \Omega_i, q, m \in \Phi_q, p \in \Psi_{q_m}$$

$$\text{(A18)}\qquad F_{i,q} \ge F_{j,q} + \mathrm{TT}_{j,q_{(m,p)-1}} + \frac{d_{j,i} - \mathrm{TL}_{j,i,q_{(m,p)-1}}}{s_{j,i,q_{m,p}}} - M(1 - B_{j,i,q_{m,p}}) \quad \forall i,j \in \Omega_i, q, m \in \Phi_q, p \in \Psi_{q_m}$$

If an ignition occurs at node i, then the fire arrival time for node i is set a priori by eq. A15. We only demonstrate a single ignition point in our test cases, but the possibility of multiple ignition points is allowed for fires that are discovered after they have spread beyond the size of a single cell. If an ignition does not occur at node i, then eqs. A16, A17, and A18 work together to set the fire arrival time and corresponding binding fire spread path. The auxiliary variable $A_{j,i,q_{m,p}}$ indicates the first subscenario $q_{m,p}$ in which the distance the fire traveled from node j to node i exceeds the distance between the nodes. Equation A16 requires that this auxiliary variable take a value of one in the first subscenario $q_{m,p}$ in which the distance the fire could have traveled from node j to unsuppressed node i is greater than the total distance between the nodes. This activates eq. A17, which requires the arrival time for node i to be less than or equal to all possible arrival times from each neighboring node. Equation A18 can only be feasible if the binding spread path from node j to node i corresponds to the earliest fire arrival time. It is because of eq. A18 that we must include a decision variable for each spread path in every subscenario: if we only had a set of spread path decision variables for each scenario, eq. A18 would be infeasible in the subscenarios prior to fire actually arriving at a node.

$$\text{(A19)}\qquad F_{i,q} \ge \sum_{k=1}^{m}\sum_{r=1}^{p} t_{q_{k,r}} - M\left(\sum_{k=1}^{m}\sum_{r=1}^{p} D_{i,q_{k,r}}\right) \quad \forall i, q, m \in \Phi_q, p \in \Psi_{q_m}$$

$$\text{(A20)}\qquad F_{i,q} \le \sum_{k=1}^{m}\sum_{r=1}^{p} t_{q_{k,r}} + M\left(1 - \sum_{k=1}^{m}\sum_{r=1}^{p} D_{i,q_{k,r}}\right) \quad \forall i, q, m \in \Phi_q, p \in \Psi_{q_m}$$

Equations A19 and A20 link the fire arrival time at each node to the subscenario in which fire arrives at each node. For subscenarios that occur before fire arrives at node i, eq. A19 ensures that node i cannot burn. Once the subscenario in which the fire arrives at node i occurs, then eq. A20 requires the decision variable indicating node i burned in subscenario $q_{m,p}$ to be one. Because (*i*) fire arrival times for ignitions are set explicitly by eq. A15 and (*ii*) eqs. A19 and A20 require a binding ignition time to be associated with the stage at which the node burned, it is not feasible for suppression to be placed at nodes at which exogenous ignitions occur.

The constraints outlined in the above sections are a complete set of fire growth equations. These constraints solved simultaneously provide a prediction of when fire will arrive at each node in a landscape. In the following sections, we add fireline intensity to the reported fire behavior and discuss constraints to govern the suppression nodes.

Fireline intensity constraints

Fireline intensity is dependent on the binding fire spread path to each node, thus accounting for terrain and fuel effects, and on the weather subscenario in which the node was ignited.

$$\text{(A21)}\qquad I_{i,q} = \sum_{m\in\Phi\_q}\sum_{p\in\Psi_{q_m}}\left(\kappa_{i,q_{m,p}} s_{i,q_{m,p}} + \sum_{j\in\Omega_i} \kappa_{j,i,q_{m,p}} B_{j,i,q_{m,p}}\right) \quad \forall i, q$$

The fireline intensity at which a node burned is set using eq. A21. All the possible fireline intensities at which node i could burn are calculated as parameters before the optimization model is run (i.e., $\kappa_{j,i,q_{m,p}}$ and $\kappa_{i,q_{m,p}}$).

Suppression constraints

We use suppression nodes in this paper as a mechanism to test how suppression could be incorporated into the model to influence fire behavior. We model these suppression nodes such that they are implemented and assumed effective immediately at the beginning of each decision stage. If such suppression nodes are spatially unconstrained and the objective is to minimize expected area impacted by fire and suppression, then suppression always would be placed in all the cells adjacent to any ignition node, making the suppression node placement decisions trivial. To avoid this and to reflect issues such as the time required to implement suppression, we identify in eq. A22 a total number of nodes in which suppression may be completed for each decision stage.

$$\text{(A22)}\qquad \sum_i Y_{i,q_m} \le c_{q_m} \quad \forall q, m \in \Phi_q$$

Nonanticipativity constraints are given in the following equation and are further discussed in the text of the paper.

$$\text{(A23)}\qquad Y_{i,q_k} = Y_{i,q_m} \quad \forall i,\ q_m \text{ and } q_k \text{ occuring after a common decision point}$$

Objective function

We used the following objective function to minimize the total expected area impacted by fire and suppression activity for the test cases presented in the results section.

$$\text{(A24)} \qquad \min E[Z] = \sum_{q} \Pr[q] \left(\sum_{m \in \Phi_q} \sum_{i} \left(Y_{i,q_m} + \sum_{p \in \Psi_{q_m}} D_{i,q_{m,p}} \right) \right)$$

Equation A24 minimizes total expected burned area plus the total expected area affected by suppression operations ($E[Z]$). In this formulation, Z is the total area impacted by fire and suppression. It is necessary to include the nodes burned in the terminal subscenarios ($q_{p\sim}$) in this objective function, as we would like the solution to fully contain the fire. If these nodes are not included, then the optimal solution may minimize fire spread during the planning horizon without containing the fire, allowing the fire to continue spreading after the planning horizon has ended.